Turbulence and radial electric field asymmetries measured at TJ-II plasmas

T. Estrada[1], E. Sánchez[1], J. M. García-Regaña[1], J. A. Alonso[1], E. Ascasíbar[1], I. Calvo[1], A. Cappa[1], D. Carralero[1], C. Hidalgo[1], M. Liniers[1], I. Pastor[1], J. L. Velasco[1] and the TJ-II team[1]

[1]Laboratorio Nacional de Fusión. CIEMAT, 28040 Madrid, Spain

Email contact main author: teresa.estrada@ciemat.es

Abstract: Dedicated experiments have been carried out for a systematic comparison of turbulence wavenumber spectra and perpendicular rotation velocity measured at poloidally separated positions in the same flux-surface in the stellarator TJ-II. The rationale behind this study is twofold, verification of the spatial localization of instabilities predicted by the gyrokinetic simulations in stellarators and verification of the electrostatic potential variation on the flux surface as calculated by neoclassical codes and its possible impact on the radial electric field. Perpendicular wavenumber spectra and perpendicular rotation velocity profiles have been measured using Doppler reflectometry in two plasma regions poloidally separated. A systematic comparison between the measurements has been carried out showing differences in the perpendicular wavenumber spectrum measured at poloidally separated positions in the same flux-surface, that depend on plasma density, heating conditions and magnetic configuration. The asymmetry found in the standard magnetic configuration under some plasmas conditions, reverses in a high iota configuration. The different intensity in the density fluctuation spectra can be related to the poloidal localization of instabilities found in the gyrokinetic simulations. Differences in the perpendicular rotation velocity and radial electric field profiles are also found that could be explained to be due to plasma potential variations within the flux surfaces

1. Introduction

The transport in magnetically confined fusion plasmas can be largely determined by turbulence. The appropriate framework to study plasma turbulence is the gyrokinetic formalism, which makes kinetic simulations with codes based on it affordable. However, these codes should be carefully validated against experiment in order to be useful for actual prediction. Scale resolved turbulence measurements are important in order to identify the type of turbulence and for the validation of turbulence simulations. In stellarators gyrokinetic simulations show a distribution of the turbulence fluctuations on the magnetic surfaces that differs from that in tokamaks [1, 2, 3, 4]. The geometric properties of the field lines vary greatly over the magnetic surfaces and unstable modes have the maximum amplitude in locations of bad magnetic field line curvature and small local magnetic shear. In TJ-II, gyrokinetic simulations show that the electrostatic instabilities (ITG, TEM and ETG) are localized in narrow stripes along certain magnetic field lines [5]. The predicted localization of instabilities has motivated a number of experiments in TJ-II for a systematic comparison of the perpendicular wavenumber spectra measured at two poloidally separated positions using Doppler reflectometry.

On the other hand, in stellarators it is the neoclassical transport that determines the radial electric field. In most cases, neoclassical calculations only consider the lowest order electrostatic potential that only depends on the flux surface label. However, variations of the neoclassical electrostatic potential over the flux surface can be relatively large under certain plasma conditions, namely at low collisionalities [6]. At TJ-II, observations of potential variations along the flux surfaces, measured using two distant Langmuir probe arrays, have been previously reported [7]. Differences in the edge floating potentials

profiles of several tens of volts were measured in low density plasmas in agreement with the overall variation in potential obtained in the neoclassical simulations. The relevance of this potential variation lies in its effect on the neoclassical impurity transport [8, 9]. In addition, the electrostatic potential variation on the flux surface may impact the radial electric field through its radial variation. This possible impact has been studied by the comparison between the perpendicular rotation velocity of the plasma turbulence, that in general is dominated by the $E \times B$ velocity, measured at two poloidally separated positions using Doppler reflectometry.

Doppler Reflectometry makes use of a finite tilt angle between the probing beam and the cut-off layer normal to measure the Bragg back-scattered process that takes place at the cut-off layer. This technique allows the measurement of the density turbulence and its perpendicular rotation velocity, at different turbulence scales and with good spatial and temporal resolution [10, 11, 12, 13]. In particular, the Doppler Reflectometer (DR) in operation at TJ-II allows measuring at two plasma regions poloidally separated [14].

Dedicated experiments have been carried out in different plasma scenarios for a systematic comparison of the Doppler reflectometer measurements −perpendicular wavenumber spectrum and perpendicular rotation velocity− at poloidally separated positions in the same flux-surface.

The remainder of the paper is organized as follows. The Doppler reflectometer measurement capabilities are described in section 2 and the experimental results in section 3. Finally, the summary is included in sections 4.

2. Experimental set-up

TJ-II is a helical device with major radius $R = 1.5$ m, minor radius $a \leq 0.22$ m and magnetic field $B_0 \leq 1.2$ T. TJ-II offers the possibility to explore a wide rotational transform range in low, negative magnetic shear configurations. Plasmas are created and heated by ECH 2^{nd} harmonic using two gyrotrons at 53.2 GHz with X-mode polarization and a maximum power per gyrotron of 300 kW. Under ECH heating conditions the plasma density has to be kept below the cut-off value of 1.75×10^{19} m^{-3}. Higher density plasmas are achieved using NBI heating. Two injectors, one co- and one counter-, are in operation delivering a port-through power per injector up to 700 kW [15].

Doppler Reflectometry is used to measure the density fluctuations and its perpendicular rotation velocity, at different spatial scales and with good spatial and temporal resolution. In TJ-II, an optimized Doppler Reflectometer (DR) is in operation since 2009 [14]. The reflectometer works in a frequency hopping mode in the Q-band: $33 - 50$ GHz, covering typically the radial region from $\rho \sim 0.6$ to 0.9. Its in-vessel front-end consist of a compact corrugated antenna and an ellipsoidal mirror that focus the probing microwave beam to the cut-off layer with a well defined optimized beam waist. The mirror can be tilted to probe different perpendicular wave-numbers of the turbulence, covering the range: $k_\perp = 1 - 14$ cm^{-1}. This $\rho - k_\perp$ parameter range can be explored in two plasma regions poloidally separated as illustrated in figure 1. In the following, the region on the left of the figure will be called *region_1* and that on the right *region_2*. The perpendicular rotation velocity of the plasma turbulence measured by Doppler reflectometry is a composition of both the plasma $E \times B$ velocity and the intrinsic phase velocity of the density fluctuations: $u_\perp = v_{E\times B} + v_{ph}$. In cases in which the condition $v_{E\times B} >> v_{ph}$ holds, E_r can be obtained directly from the perpendicular rotation velocity: $E_r = u_\perp B$. In TJ-II, previous measurements carried out in ECH and NBI plasmas support the conclusion that

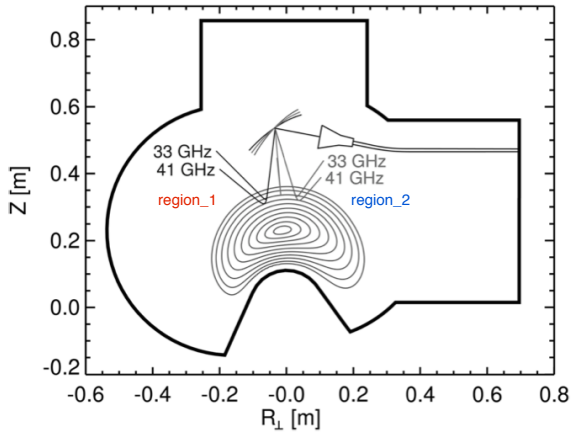

FIG. 1: Schematic representation of the TJ-II vacuum vessel with the DR antenna-mirror arrangement showing the two poloidally separated plasma regions that can be probed.

$v_{E\times B} >> v_{ph}$ allowing, in those cases, the determination of E_r [13].

3. Experimental results

3.1 Perpendicular wavenumber spectra

A set of experiments with the goal of characterizing the turbulence under different regimes in TJ-II have been carried out during the last TJ-II campaigns. Different plasmas scenarios have been studied with different plasma profile shapes, namely, high power on-axis ECH heated plasmas vs. low power off-axis ECH heated plasmas; ECH vs. NBI heated plasmas; standard vs. high rotational transform magnetic configurations. In all cases, scale-resolved density fluctuation spectra have been measured at different radial positions and in the two poloidally separated plasma regions.

3.1.1 Standard magnetic configuration

As first scenario, on-axis ECH-heated low-density plasma (with $n_e = 0.5 \times 10^{19}$ m^{-3} and $P_{ECH} = 500$ kW) in the standard magnetic configuration (rotational transform at the plasma edge: $\iota_a = 1.63$), is selected. The central electron and ion temperature are respectively $T_e(0) = 1.5$ keV and $T_i(0) = 100$ eV. A series of plasma discharges with the same plasma conditions is carried out. In each discharge the DR probing frequencies are changed to probe different radial positions while the probing beam angle is scanned in a shot to shot basis. The $k_\perp$ spectra measured by the DR in the two poloidally separated plasma regions is shown in figure 2 (*region_1* left in red and *region_2* right in blue). The spectra are measured at $\rho = 0.78 \pm 0.04$ (figure 2.a) and at $\rho = 0.69 \pm 0.04$ (figure 2.b), respectively. An asymmetry is clearly observed in the intensity of the density fluctuations in the whole $k_\perp$ range. Higher turbulence level is measured in *region_1* as compared with that measured in *region_2*, being the difference more pronounced in the outer radial position, i.e. at $\rho = 0.78 \pm 0.04$, and at intermediate turbulence scales, i.e. $k_\perp \sim 4 - 7$ cm^{-1} (figure 2.a). At the inner radial position the turbulence level measured in *region_1* decreases getting closer to the level measured in *region_2* (figure 2.b). This result is consistent with a turbulence drive radially localized closer to the outer position

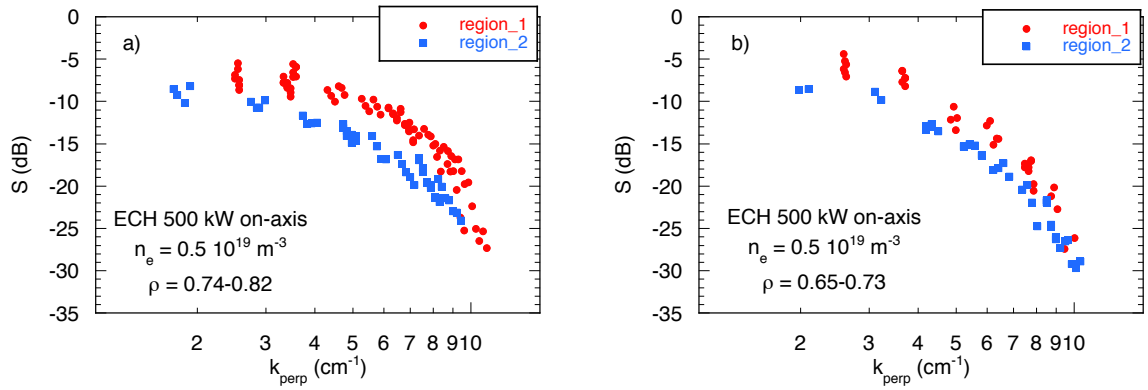

FIG. 2: $k_\perp$ spectra measured in the two plasma regions poloidally separated (region_1 in red and region_2 in blue) at $\rho = 0.78 \pm 0.04$ (a) and at $\rho = 0.69 \pm 0.04$ (b). $P_{ECH} = 500$ kW on-axis, standard magnetic configuration.

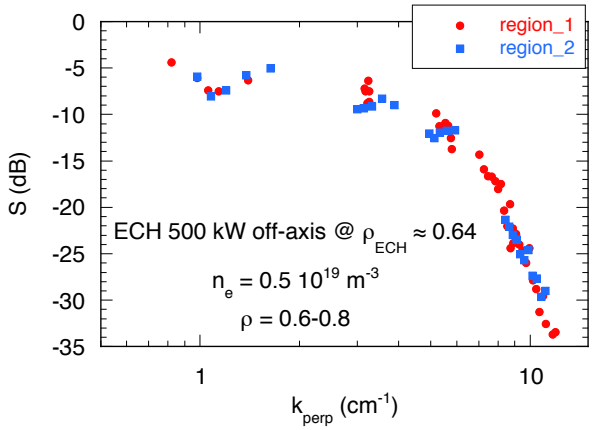

FIG. 3: $k_\perp$ spectra measured in the two plasma regions (region_1 in red and region_2 in blue) at $\rho = 0.7 \pm 0.1$. $P_{ECH} = 500$ kW off-axis, standard magnetic configuration.

of measurement than to the inner one and asymmetrically distributed over the magnetic surface.

The poloidal asymmetry discovered in the first scenario is not found when comparing the perpendicular wavenumber spectra measured in similar low density ECH plasmas in which the ECH power is deposited off-axis at $\rho_{ECH} = 0.64$. In this second scenario, the electron temperature profile is rather flat with $T_e(0) = 1.0$ keV, and $T_i(0) = 75$ eV. The $k_\perp$ spectra measured in the radial range $\rho = 0.6 - 0.8$ are shown in figure 3. Very similar density turbulence level is measured in the two poloidal regions.

In order to compare with these experimental results, global gyrokinetic simulations using the code EUTERPE [16, 2] are being performed [5, 17]. Linear analyses of instabilities have been done considering kinetic ions and electrons, collisions, and experimental density, temperature and radial electric field profiles. The instabilities are driven by the electron temperature gradient and the main contribution comes from the ∇B term, compatible with Trapped Electron Modes (TEM). The details of these simulations are described in [17]. Differences in the radial localization of the most unstable modes are found when comparing the two plasma scenarios, which are consistent with the dependences found in the experiments. Regarding the turbulence localization along the flux surface, an asymmetry is also observed in the simulations, however, a quantitative agree-

ment with the experiments has not been found yet. Non-linear simulations are in progress to proceed with the simulation & experiment comparisons.

A third scenario with higher density plasmas ($n_e = 1.2 \times 10^{19}$ m^{-3}) heated with lower ECH power ($P_{ECH} = 250$ kW) deposited off-axis at $\rho_{ECH} = 0.4$, has been also explored. Under these conditions, $T_i(0) = 90$ eV and lower electron temperatures are measured (about $0.3 - 0.4$ keV) with slightly hollow profiles. In these plasmas the collisionality is higher than in the previous scenarios and E_r is negative in the whole plasma column, i.e. the plasma is in the neoclassical ion root confinement regime. A poloidal asymmetry in the $k_\perp$ spectra is found with a behaviour that resembles that found in the first scenario, i.e., higher turbulence level in *region_1* as compared with *region_2*.

Similar plasma parameters as those in the third scenario are measured when heating with only NBI at moderate plasma densities ($n_e = 1.0 \times 10^{19}$ m^{-3}). With a port-through power of $P_{NBI} = 500$ kW, flat temperature profiles are measured with $T_e(0) = 0.4$ keV, and $T_i(0) = 120$ eV. This fourth scenario has been also investigated searching for poloidal asymmetries in the plasma turbulence. As in the first and third scenarios, higher turbulence level is measured in *region_1* as compared with *region_2*.

3.1.2 Magnetic configuration with high rotational transform

A magnetic configuration with higher rotational transform ($\iota_a = 2.24$) has been studied under the same experimental conditions as in the first scenario: on-axis ECH-heated low-density plasma (with $n_e = 0.5 \times 10^{19}$ m^{-3} and $P_{ECH} = 500$ kW). As for the first scenario in the standard magnetic configuration, the electron temperature profile is peaked with central values of $T_e(0) = 1.5$ keV, and $T_e(0) = 100$ eV. The perpendicular wavenumber spectra measured in the two poloidally separated plasma regions are shown in figure 4. The spectra in this high ι configuration are measured at $\rho = 0.81 \pm 0.05$ (figure 4.a) and at $\rho = 0.71 \pm 0.05$ (figure 4.b), and as in the standard magnetic configuration, a poloidal asymmetry in the perpendicular wavenumber spectra is found. However in this magnetic configuration, the turbulence level is higher in *region_2* as compared with *region_1*. It is worth mentioning that, as for the data recorder so far, this reversal in the poloidal asymmetry is specific of this magnetic configuration with high rotational transform.

The influence of the rotational transform on the turbulence localization along the flux surface has been also studied by gyrokinetic simulations. The maximum amplitude of the instabilities is displaced poloidally when the rotational transform is increased as observed in the experiments. However, a quantitative agreement with the experiments has not been found yet.

3.2 Perpendicular rotation velocity

Different plasma conditions have been explored searching for poloidal asymmetries in the perpendicular rotation velocity of the plasma turbulence measured by DR.

The most pronounced poloidal asymmetries are found in low density plasmas in the neoclassical electron root confinement regime. In TJ-II, the transition from the electron to the ion root takes place when the density exceeds some critical value that depends on the heating power and plasma volume [18]. Below the critical density, E_r is positive in the whole plasma column, and as the density approaches the critical value, the inversion in E_r is observed; the inversion starts in the region of maximum density gradient and expands radially in agreement with neoclassical calculations [19, 20]. The perpendicular rotation

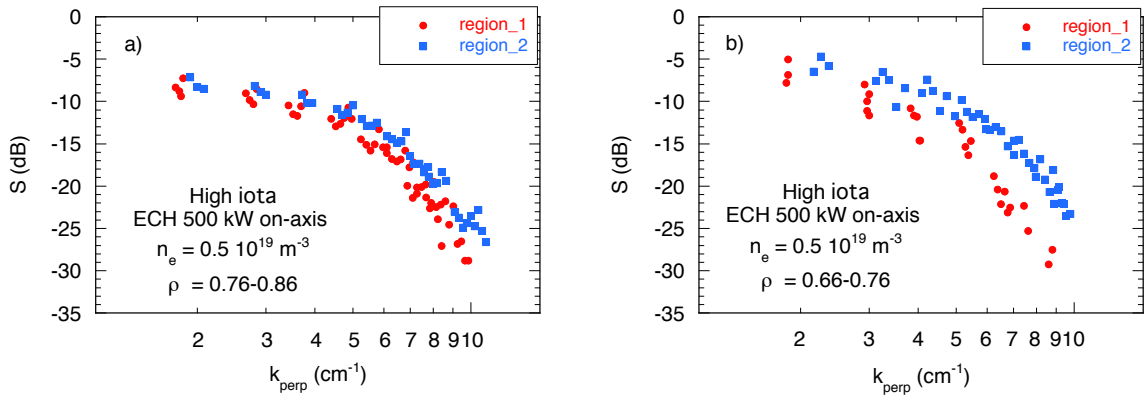

FIG. 4: $k_\perp$ spectra measured in the two plasma regions (region_1 in red and region_2 in blue) at $\rho = 0.81 \pm 0.05$ (a) and at $\rho = 0.71 \pm 0.05$ (b). $P_{ECH} = 500$ kW on-axis, high rotational transform magnetic configuration.

velocity measured at the two poloidal regions shows pronounced differences in low density plasmas, i.e. in neoclassical electron root confinement regime. An example is shown in figure 5. The $u_\perp$ profiles measured at turbulence scales in the range $k_\perp \sim 6 - 8$ cm^{-1}, in the two poloidal plasma regions (*region_1* in red and *region_2* in blue) for plasmas in electron and ion root confinement regimes are shown together with the corresponding electron density profiles. At low densities, a pronounced poloidal asymmetry is found in the rotation velocity over the radial range $\rho \sim 0.6 - 0.8$. Under the same heating conditions, a slight increase in the density produces the inversion in $u_\perp$. In this case, the poloidal asymmetry in $u_\perp$ is lost and the profiles measured in the two poloidal plasma regions overlap to each other (open symbols in figure 5.left). The poloidal asymmetry in $u_\perp$ in the electron root confinement regime is found both in Hydrogen and Deuterium plasmas, in the standard magnetic configuration. Similar values of $u_\perp$ are found in the magnetic configuration with high rotational transform for the same heating conditions. However, as for the fluctuation level, the asymmetry in $u_\perp$ reverses and $u_\perp$ in *region_1* is higher than $u_\perp$ in *region_2*.

Assuming that $u_\perp$ is dominated by the $v_{E\times B}$, i.e. that the intrinsic phase velocity of the turbulence is negligible, the asymmetry in $u_\perp$ found in the electron root confinement regime in the standard magnetic configuration yields differences in E_r of about 1 kV/m. Two experimental observations support the assumption: $v_{E\times B} >> v_{ph}$ in these plasma conditions: on the one hand, the good agreement between the E_r profiles measured using HIBP and DR in low density electron root plasmas [13, 5], and on the other hand, the lack of dependence of $u_\perp$ on the turbulence scale, $k_\perp$. This is illustrated in figure 6. It shows $u_\perp$ plotted as a function of ρ (figure 6.a) and as a function of $k_\perp$ (figure 6.b). The data was measured in the first scenario described in section 3.1.1. $u_\perp$ increases from 1 to 4 km/s in the radial range $\rho \sim 0.6 - 0.8$ and no clear trend is found in the $u_\perp$ vs. $k_\perp$ representation, indicating that all turbulence scales propagate at the same velocity that only depends on the radial position. Only the data measured in the poloidal *region_2* is shown in figure 6 but the same conclusion can be derived from the data measured in *region_1*. This result allows us to conclude that the intrinsic phase velocity of the plasma turbulence, that naturally depends on $k_\perp$ via the dispersion relation, should be negligible as compared with $v_{E\times B}$. It is worth mentioning that this behaviour is not observed for some specific plasma conditions and therefore it cannot be generalized.

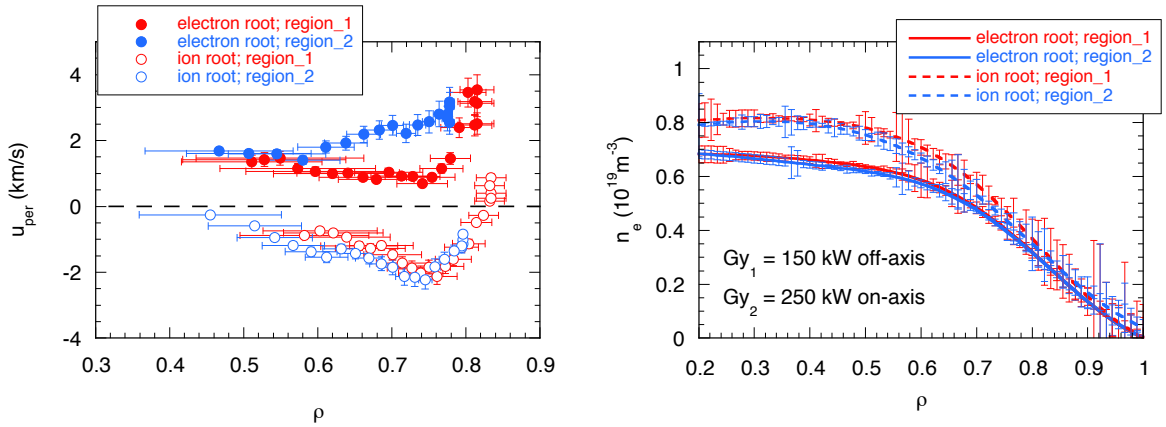

FIG. 5: Left: $u_\perp$ profiles measured by the DR at turbulence scales $k_\perp \sim 6-8\ cm^{-1}$, in the two plasma regions (region_1 in red and region_2 in blue) in both electron and ion root regimes. Right: density profiles measured in these discharges. ECH plasmas in the standard magnetic configuration.

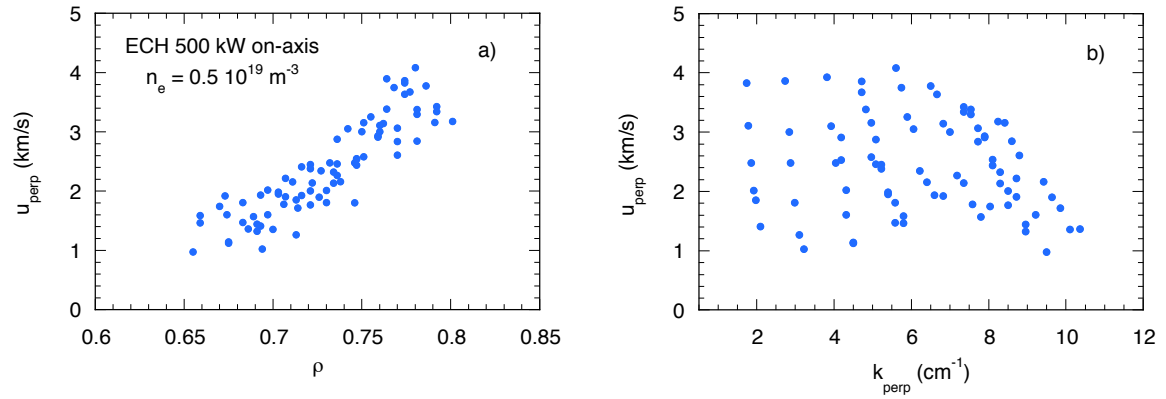

FIG. 6: $u_\perp$ measured by the DR in the poloidal region_2 in the electron root regime, as a function of ρ (a) and $k_\perp$ (b), in the standard magnetic configuration.

The rather large poloidal asymmetry in E_r found experimentally in the electron root regime as well as the lack of asymmetry found in the ion root regime (figure 5.left), motivated the numerical analysis of the radial electric field taking into account the contribution arising from the radial dependence of the neoclassical electrostatic potential variation along several flux surfaces. For the analysis, the neoclassical version of the code EUTERPE was used taking into account the experimental plasma profiles. The results show variations in E_r comparable to those found in the experiments [21]. The contribution from the neoclassical electrostatic potential varying within the flux surfaces introduces an asymmetry in E_r that is a significant fraction of the ambipolar E_r in the electron root regime and much smaller in the ion root regime. It should be mentioned, however, a disagreement regarding the sign of the E_r correction when simulations and experiments are compared.

4. Summary

A systematic comparison of turbulence wavenumber spectrum and perpendicular rotation velocity measured using Doppler reflectometry at poloidally separated positions in the same flux-surface, has been carried out in the stellarator TJ-II. Poloidal asymmetries

in the $k_\perp$ spectrum are found that depend on plasma density, heating conditions and magnetic configuration. In the standard magnetic configuration, the strongest poloidal asymmetry is found in plasma scenarios with high electron temperature gradients at the plasma edge. This asymmetry reverses in the magnetic configuration with high rotational transform. These results are in good qualitative agreement with the spatial localization of instabilities as calculated using the global gyrokinetic code EUTERPE in TJ-II plasmas [17]. The most pronounced poloidal asymmetries in E_r are found in low density plasmas in the neoclassical electron root confinement regime, in both Hydrogen and Deuterium plasmas, in the standard magnetic configuration. Similar values of E_r are found in the magnetic configuration with high rotational transform however, as for the turbulence spectrum, the asymmetry in E_r reverses. The asymmetry in the E_r profile can be explained to be due to the radial dependence of electrostatic potential varying over the flux surface [21].

Acknowledgements

The authors acknowledge the entire TJ-II team for their support. This work has been partially funded by the Spanish Ministry of Science and Innovation under contract numbers FIS2017-88892-P and ENE2015-70142-P. This work has been carried out within the framework of the EUROfusion Consortium and has received funding from the Euratom research and training programme 2014-2018 under grant agreement No 633053. The views and opinions expressed herein do not necessarily reflect those of the European Commission.

References

[1] M. Nadeem, T. Rafiq, and M. Persson, Physics of Plasmas **8**, 4375 (2001).
[2] V. Kornilov *et al.*, Physics of Plasmas **11**, 3196 (2004).
[3] P. Xanthopoulos, G. G. Plunk, A. Zocco, and P. Helander, Phys. Rev. X **6**, 021033 (2016).
[4] E. Sánchez, (43rd EPS Conference on Plasma Physics, Leuven, Belgium, 2016).
[5] E. Sánchez, (21st International Stellarator/Heliotron Workshop, Kyoto, Japan, 2017).
[6] D. D. Ho and R. M. Kulsrud, The Physics of Fluids **30**, 442 (1987).
[7] M. A. Pedrosa *et al.*, Nuclear Fusion **55**, 052001 (2015).
[8] J. M. García-Regaña *et al.*, Plasma Physics and Controlled Fusion **55**, 074008 (2013).
[9] J. M. García-Regaña *et al.*, Nuclear Fusion **57**, 056004 (2017).
[10] M. Hirsch *et al.*, Plasma Physics and Controlled Fusion **43**, 1641 (2001).
[11] P. Hennequin *et al.*, Rev. Sci. Instrum. **75**, 3881 (2004).
[12] G. D. Conway *et al.*, Plasma Physics and Controlled Fusion **46**, 951 (2004).
[13] T. Estrada *et al.*, Plasma Phys. Control. Fusion **51**, 124015 (2009).
[14] T. Happel *et al.*, Rev. Sci. Instrum. **80**, 073502 (2009).
[15] M. Liniers and J. Alonso, Fusion Technology **1**, 307 (1998).
[16] G. Jost *et al.*, Physics of Plasmas **8**, 3321 (2001).
[17] E. Sánchez *et al.*, (27th IAEA FEC, EX/P1-11, Ahmedabad, India, 2018).
[18] L. Guimarais *et al.*, Plasma and Fusion Research **3**, S1057 (2008).
[19] T. Happel, T. Estrada, and C. Hidalgo, Eur. Phys. Lett. **84**, 65001 (2008).
[20] J. L. Velasco *et al.*, Plasma Physics and Controlled Fusion **55**, 124044 (2013).
[21] J. M. García-Regaña *et al.*, Plasma Physics and Controlled Fusion **60**, 104002 (2018).